

1 **Key evidence for distal turbiditic- and bottom-current interactions from**
2 **tubular turbidite infills**

3

4 Francisco J. Rodríguez-Tovar^{1,*}, Francisco J. Hernández-Molina², Heiko Hüneke³, Domenico
5 Chiarella², Estefanía Llave⁴, Anxo Mena⁵, Olmo Miguez-Salas¹, Javier Dorador², Sandra de
6 Castro², Dorrik A.V. Stow⁶

7

8 ¹ Dept. Estratigrafía y Paleontología, Universidad de Granada, 18002 Granada, Spain

9 ² Dept. Earth Sciences, Royal Holloway Univ. London, Egham, Surrey TW20 0EX, UK

10 ³ Institut für Geographie und Geologie, Universität Greifswald, D-17487 Greifswald, Germany

11 ⁴ Instituto Geológico y Minero de España, 28003 Madrid, Spain

12 ⁵ Dept. Xeociencias Mariñas e O.T., Universidade de Vigo, 36310 Vigo, Spain

13 ⁶ Heriot-Watt University, Edinburg, Edinburgh EH14 4AS, Scotland, UK

14

15 * Corresponding author

16

17

18

19 **ABSTRACT**

20 Infilling of trace fossils can serve as a proxy for sediment otherwise missing from basin
21 deposits. The Petra Tou Romiou section (southern Cyprus) includes calcilutite/calcarenite
22 material that represents deep-marine deposits of Eocene age. Lateral and vertical variation
23 indicates pelagic, gravitational, and bottom-current processes simultaneously influencing
24 sedimentation. Detailed ichnological analysis resolved interactions between these deep-marine
25 sedimentary processes in this distal marine setting. Calcarenite turbiditic beds occur as well-
26 preserved and continuous tabular beds that disappear laterally. In some cases, trace fossils
27 infilled with calcarenitic material are termed *tubular turbidites*. These structures correspond to
28 actively filled *Planolites* formed in softground conditions and infilled by calcarenitic sediment
29 interpreted as the record of missing turbiditic deposits when calcarenite turbiditic beds
30 disappeared due to erosion. The variable preservation of calcarenite turbidite beds along with the
31 presences of *tubular turbidites* indicate rapid erosion following turbidite deposition and post-
32 depositional reworking of turbidites by bottom-currents. A refined interpretation of *tubular*
33 *turbidites* can help constrain sedimentary processes that form deep-marine deposits and as such,
34 has considerable paleoceanographic and economic implications.

35

36 *Keywords:* Trace fossils, *Planolites* infill, turbidites, contourites, Petra Tou Romiou, Cyprus

37

38 **1. Introduction**

39

40 Deep-marine settings consist of deposits influenced by three main sedimentary processes
41 including pelagic (vertical settling of pelagic particles in the water column), gravitational
42 (downslope density currents; turbid flows of predominantly terrigenous sediments), and bottom
43 current (mainly alongslope flow of bottom currents) (e.g., Rebesco et al., 2014). End-member
44 deposits in these settings may arise from a single, predominant process, while more varied
45 deposits can form due to the interaction of processes (e.g., Pickering and Hiscott, 2016).
46 Gravitational currents and overflows, together with barotropic currents, giant eddies, deep-sea
47 storms, vortices, internal waves, internal tides, or tsunamis, among other processes, can all affect
48 the seafloor in deep-water environments (see Fig. 13 in Rebesco et al., 2014). Over the last
49 decade, studies of different continental margins have described how these processes in

50 combination can result in mixed / hybrid sedimentary systems (Gong et al., 2018; Sansom, 2018;
51 Normandeau et al., 2019). Differentiation of gravitational and bottom-current processes remains
52 a challenge however. Without clearly delineated examples, these systems are difficult to interpret
53 in terms of standard turbiditic and contourite facies models (Shanmugam, 2002; Rebesco et al.,
54 2014).

55 Ichnological analysis is a useful tool for identifying and characterizing pelagic,
56 gravitational, and bottom current deposits (Wetzel et al., 2008; Rodríguez-Tovar and Hernández-
57 Molina, 2018; Rodríguez-Tovar et al., 2019a). Infilling of trace fossils can provide key evidence
58 of sediment lost from shallow- to deep-marine environments (i.e., Wetzel, 2015). In some cases,
59 the sedimentary record is preserved exclusively by burrow infill. Fill was emplaced deep within
60 the surrounding sediment and can thereby elude mixing by bioturbation or later erosion. Both
61 actively and passively filled burrows can store sediment not otherwise preserved. Three different
62 cases have been proposed based on type of infilling material and depositional processes: *tubular*
63 *tempestites* (Wanless et al., 1988; Gingras et al., 2007; Leonowicz, 2016); *tubular tidalites*
64 (Gingras and MacEachern, 2012; Wetzel et al., 2014; Gingras and Zonneveld, 2015; Rodríguez-
65 Tovar et al., 2019b), and *tubular turbidites* (Hubbard et al., 2012). These latter deposits were
66 described by Hubbard et al. (2012) as follows: “sand-filled burrows (in some instances) record
67 the passage of coarse-grained material through an erosional conduit such as a submarine canyon
68 or channel, without deposition of a coarse lag,” wherein “the only evidence of coarse-grained
69 sediment in the system may be recorded within the burrow fills”. In this interpretation, *tubular*
70 *turbidite* means passively filled firmground burrows in the bathyal realm, belonging to the
71 *Glossifungites* ichnofacies, and indicating sediment bypass.

72 This contribution describes a new type of *tubular turbidites* associated to actively infilled
73 *Planolites* produced in softgrounds and reflecting varying degrees of post-depositional erosion
74 by bottom-current activity, from the Eocene Lefkara Formation of the Petra Tou Romiou section
75 (southern Cyprus, Eastern Mediterranean Sea: Fig. 1). The Lefkara *tubular turbidites* consist of
76 actively filled softground burrows and associate with calcarenite sediments subjected to different
77 degrees of erosion. As such, these features provide key evidence of turbiditic- and bottom-
78 current interactions which can ultimately inform sedimentary interpretations, paleoclimatic
79 research, and petroleum exploration.

80

81 2. Geological setting and the studied section

82

83 The Petra Tou Romiou section is located in an outcrop at the southern part of Cyprus,
84 Eastern Mediterranean Sea (34°39'27.4''N, 32°38'55.5''E). It includes both the Lefkara and
85 Pakhna formations, which are part of the Circum Troodos Massif sedimentary succession
86 (Edwards et al., 2010) (Fig. 1). The research is conducted at the Lefkara Formation (late
87 Palaeocene to Oligocene), which consists primarily of chalky limestones and marls with
88 intercalated bedded and nodular cherts (Edwards et al., 2010). This carbonate-dominated
89 succession formed by pelagic and hemipelagic sediment accumulation temporarily influenced by
90 weak bottom-currents and punctuated by distal turbidity flows (Stow et al., 2002). The
91 depositional setting of this deep-marine record developed along the lower continental slope
92 during the Eocene. The Parkhna Formation, overlying the Lefkara Formation disconformably in
93 most areas, consists of chalks, marly chalks, bioturbated silty marls to siltstones, calcarenites and
94 conglomerates, deposited during the Miocene (Eaton and Robertson, 1993).

95 The lower part of the studied Lefkara Formation belongs to the Chalk Unit, consisting of
96 regular alternation of calcilutites and calcarenite beds (Fig. 2). Whitish calcilutites consisting of
97 globigerinid wackestones (sparse biomicrites) reach thicknesses of a meter to several meters and
98 represent the primary lithology (Fig. 2). These whitish calcilutites can exhibit decimetre-scale
99 banding marked by subtle color changes. Thin, interbedded calcarenites (thicknesses < 5 cm)
100 consist of globigerinid wackestones-packstones and show transitional relationships with the
101 whitish calcilutites. In some cases, thicker interbedded calcarenites (5-8 cm) exhibit faint wavy
102 lamination (calnwl in Fig. 3A-D). A second type of calcarenite beds show a sharp base and
103 exhibit pronounced normal grading. These beds shift from parallel- and cross-laminated to
104 bioturbated fabrics (Fig. 3D). Some of the more coarse-grained beds from this facies show good
105 lateral continuity (caln in Fig. 3) while others may thin out and even disappear laterally (caln-d
106 in Fig. 3). This transition leaves a subtle pressure dissolution seam (Figs. 3C). In some cases, a
107 vertical calcilutite-calcarenite-calcilutite succession consisting of whitish calcilutites, well-
108 developed calcarenite beds, whitish calcarenites with faint wavy lamination and then whitish
109 calcilutites is observed (Fig. 3).

110

111 3. Methods

112

113 During five field campaigns (2014 to 2018) *The Drifters Research Group* (RHUL) and
114 the *Ichnology & Palaeoenvironment Research Group* (UGR) have been studying Eocene to early
115 Miocene succession from Lefkara and Pakhna formations (Cyprus). Detailed sedimentological
116 and ichnological analysis of the Lefkara Formation focussed especially on the transition between
117 calcilutites and well-defined (sharp based) calcarenite beds identified as turbidites. Stratigraphic
118 and sedimentological observation documented stratigraphic architecture, contacts between
119 sedimentary facies, and lateral variation in calcarenite beds.

120 Outcrop observations of ichnological features included analysis of shape, configuration,
121 orientation, length, width, and diameter of burrows, burrow margins, and especially sediment fill
122 within trace fossils. We also analysed relationships between trace fossil assemblages and both
123 the whitish calcilutite and sharp based calcarenite facies types. Select samples were collected for
124 further imaging and petrographic analysis in laboratory.

125

126

127 **4. Ichnological analysis**

128

129 Ichnological analysis of calcilutite intervals distinguished two trace fossil assemblages
130 according to infill material (Figs. 4, 5).

131 The first is a light trace fossil assemblage with calcilutite infill primarily resembling the
132 host sediment and consisting of dominant *Chondrites* and *Planolites*, and frequent *Thalassinoides*
133 and *Zoophycos*. This assemblage occurs extensively throughout the calcilutite interval and was
134 previously described by Miguez-Salas and Rodríguez-Tovar (2018; Fig. 4). *Chondrites* is
135 observed in variably oriented vertical cross sections with oval or circular spots with burrow
136 diameters of 1-2 mm-wide (smaller forms) and 2-3 mm-wide (larger forms). *Planolites* are
137 registered as horizontal straight to gently curved flattened cylinders, and elliptical spots in cross
138 sections, unlined, showing diameters from 0.3 to 1.5 cm. *Thalassinoides* is mainly observed in
139 vertical cross sections as unlined cylindrical or subcylindrical horizontal forms, with diameters
140 ranging from 2 to 7 cm. *Zoophycos* is registered only in vertical cross sections as horizontal to
141 sub-horizontal spreiten structures, with widths between less than 10 cm to almost 30 cm.

142 The second type is a conspicuous trace fossil assemblage primarily comprised of
143 horizontal and slightly oblique bioturbation structures with calcarenite infill similar to the
144 calcarenite beds. These fossils occur exclusively in upper part of the calcilutite intervals and
145 below calcarenite beds (Fig. 5). In the second type, the trace fossils are linear, cylindrical, had a
146 smooth tubular morphology, are subcircular in cross-section, and are sometimes preserved as a
147 full-relief exichnion, 8 mm in diameter. The longest observed length up to 5 cm. The traces are
148 simple, mainly horizontal or slightly inclined and without branching. These features allow
149 assignation to *Planolites*, and differentiation respect to larger and branched structures as
150 *Thalassinoides*. Discrete calcarenite infilled trace fossils showed clear but variable relationships
151 with overlying sharp based calcarenites. These in turn allowed for differentiation of three cases
152 (Fig. 5):

- 153 i) Conspicuous calcarenite infilled trace fossils derived from a well-preserved calcarenite
154 bed, which occurred in contact with or at a short remove from the fossils (Fig. 5A, B).
155 Penetration depths of up to 4 cm indicate a clear relationship between calcarenite beds
156 and the trace fossil.
- 157 ii) Conspicuous calcarenite infilled trace fossils into the calcilutite interval, and
158 underlying a discontinuous calcarenite bed/horizon (Fig. 5C, D) or a pressure
159 dissolution seam (Fig. 5E), at a stratigraphic distance of 1 to 5 cm.
- 160 iii) Conspicuous calcarenite infilled within trace fossils penetrating calcilutite intervals
161 showing no evidence of calcarenite bed/horizon or pressure dissolution seam (Fig. 5F).

162

163 This second type (*Planolites* with calcarenite infill material) is the focus of the conducted
164 research.

165

166 **5. Discussion**

167

168 Facies, facies association, and microfacies analysis allowed general interpretation of
169 depositional processes influencing the Lefkara Formation at the Petra Tou Romiou section
170 (Cyprus). The ichnological assemblage of the calcilutite facies consists of traces with calcilutite
171 infill (*Chondrites*, *Planolites*, *Thalassinoides*, and *Zoophycos*) which are typical of the *Zoophycos*
172 ichnofacies (Miguez-Salas and Rodríguez-Tovar, 2018). Together, these indicate pelagic

173 conditions. Calcarenite beds with faint wavy lamination comprise bigradational sequences
174 similar to those defined by Gontier et al. (1984) wherein gradational boundaries relate to bottom-
175 current processes. Well-developed calcarenite beds with sharp, erosive basal surfaces, normal
176 grading, and parallel to low-angle cross lamination have been interpreted as fine-grained
177 turbidites based on their semblance to fined-grained distal turbiditic deposits described in the
178 literature (e.g., Stow and Shanmugan, 1980; Pickering and Hiscott, 2016; Hüneke et al.,
179 submitted). End member deposits exhibit both lateral and vertical variation in fine-grained
180 turbidite beds overlapped by whitish calcarenites with faint wavy lamination. These indicate
181 varying degrees of interaction between depositional and erosional processes typical of deep-sea
182 environments. Distal turbidites were reworked after deposition under the control of the bottom-
183 current activity.

184 Calcarenite infill trace fossils associates exclusively with *Planolites* in the upper part of
185 the calcilutite intervals, just below the calcarenite beds. *Planolites* is typically interpreted as an
186 actively filled (burrow fill directly emplaced by the burrower; Bromley, 1996) fodinichnion
187 produced by eurybathic vagile “worm”-like deposit-feeders in softgrounds (e.g., Osgood, 1970;
188 Pemberton and Frey, 1982; Fillion and Pickerill, 1990; Keighley and Pickerill, 1995). *Planolites*
189 represent the activity of trace makers mainly in shallow tiers, up to 1 cm below the boundary
190 surface (i.e., Rodríguez-Tovar and Uchman, 2004), but has been also assigned to midtier levels
191 (Buatois et al., 2011), in any case being a characteristic component of softgrounds (Knaust,
192 2017). The presence of softground *Planolites* actively infilled by turbiditic calcarenite material
193 indicates rapid bioturbation immediately after turbidite deposition in softground conditions.
194 *Planolites* observed storing turbiditic material, in absence of the calcarenite turbiditic bed above,
195 are herein interpreted as “*tubular turbidites*”. This represents a refined definition of *tubular*
196 *turbidites* because the original description (Hubbard et al., 2012) interpreted them as related to
197 turbiditic processes without deposition of the coarse lag, wherein firmground traces passively
198 infilled by coarse-grained sediment during bypass (Fig. 6). The example described here includes
199 coarse lag, which indicates that bypass is not a necessary preservational factor.

200 The variable relationship between calcarenite infilled *Planolites* and the overlying sharp
201 based calcarenites (cases i to iii) allows for more precise interpretation of distal turbiditic- and
202 bottom-current interactions (Figs. 5 and 7):

- 203 a) A well-preserved calcarenite bed in contact with or at a short distance from clear
204 calcarenite-filled *Planolites* (Fig. 5A, B, and Fig. 7) represents complete preservation of
205 the original turbidite (case i above) without significant erosion. Subsequent bottom-current
206 processes do not rework turbiditic deposits probably due to an interval without deposition
207 (or scarce pelagic deposition) between turbiditic deposition and subsequent bottom-current
208 reworking. This favors lithification (firmgrounds) and turbidite preservation.
- 209 b) A thin calcarenite bed/horizon (Fig. 5C, D) or a pressure dissolution seam (case ii, Fig. 5E)
210 underlain by conspicuous *Planolites* (*tubular turbidites*) represents rapid, post-depositional
211 erosion of the softground turbidite by subsequent bottom-current reworking (Fig. 7).
212 Bottom currents are interpreted as relatively weak and achieve total or limited erosion.
- 213 c) Exclusive presence of conspicuous *Planolites* (*tubular turbidites*) into the calcilitic
214 interval without a calcarenite bed/horizon or a pressure dissolution seam (case iii; Fig. 5F)
215 represents total post-depositional erosion of the softground turbidite by subsequent bottom-
216 current reworking. Pervasive, strong bottom currents leave only the *tubular turbidites*
217 behind (Fig. 7).

218
219

220 **6. Conclusions**

221

222 Facies and microfacies analysis of Eocene calcilitite/calcarenite units of the Petra Tou
223 Romiou section (southern Cyprus) record the complex history of a deep-marine depositional
224 system. The section exhibits vertical gradation from whitish calcilitites, well-developed
225 calcarenite beds, and whitish calcarenites with faint, wavy lamination to whitish calcilitites.
226 These patterns indicate varying interactions between gravitational processes, bottom-currents,
227 and pelagic sedimentation. In the absence of abundant sedimentary structures or other
228 depositional indicators, detailed ichnological analysis can reveal complex turbiditic and bottom-
229 current interactions.

230 Calcarenite infilled *Planolites* located in the upper part of the calcilitite intervals occur
231 below a well-developed calcarenite bed. In some cases these are interpreted as a new type of
232 *tubular turbidite* which indicates rapid bioturbation in softground immediately following
233 turbidite deposition, and then erosion of the turbiditic bed. Calcarenite beds varied from well-

234 preserved to absent. This variable preservation of fine-grained turbidites as well as its varying
235 relationship with calcarenite infilled *Planolites* are interpreted as reflecting varying degrees of
236 post-depositional erosion by bottom-current activity.

237 These newly constrained features can improve characterization of depositional and post-
238 depositional processes. The presence of *tubular turbidites* indicates complex interactions
239 between gravitational and bottom-current processes and constrains interpretations of
240 economically and geologically significant mixed/hybrid depositional systems.

241

242 **Acknowledgements**

243

244 We would like to thank both reviewers Dr. Baniak (BP Canada Energy Group) and Dr.
245 Uchman (Jagiellonian University) for comments and suggestions, and Editor Thierry Correge by
246 the editorial work. Funding for this research was provided by Project CGL2015-66835-P
247 (Secretaría de Estado de I+D+I, Spain), Research Group RNM-178 (Junta de Andalucía), and
248 Scientific Excellence Unit UCE-2016-05 (Universidad de Granada). The research was conducted
249 with “The Drifters” Research Group of the Royal Holloway University of London (UK) and is
250 related to the projects CTM 2012-39599-C03, CGL2016-80445-R, and CTM2016-75129-C3-1-
251 R.

252

253 **References**

254

255 Bromley, R., 1996. Trace Fossils: Biology, taphonomy and applications. Chapman & Hall, 361
256 pp.

257 Buatois, L.A., Saccavino, L.L., Zavala, C., 2011. Ichnologic signatures of hyperpycnal flow
258 deposits in Cretaceous river-dominated deltas, Austral Basin, southern Argentina. In:
259 Slatt, R.M., Zavala, C. (Eds.), Sediment transfer from shelf to deep water—Revisiting
260 the delivery system. AAPG Studies in Geology 61, pp. 153–170.

261 Constantinou, G., 1995. Geological Map of Cyprus, Scale 1/250.000. Geological Survey of
262 Cyprus, Nicosia.

263 Eaton, S., Robertson, A., 1993. The Miocene Paghna Formation, southern Cyprus and its
264 relationship to the Neogene tectonic evolution of the Eastern Mediterranean.
265 *Sedimentary Geology* 86, 273–296.

266 Edwards, S., Hudson-Edwards, K., Cann, J., Malpas, J., Xenophontos, C., 2010. *Classic Geology*
267 *in Europe 7: Cyprus*. Terra Publishing, Dunedin Academic Press Ltd., 271 pp.

268 Fillion, D., Pickerill, R.K., 1990. Ichnology of the Upper Cambrian? to Lower Ordovician Bell
269 Island and Wabana groups of eastern Newfoundland, Canada. *Palaeontographica*
270 *Canadiana* 7, 1–119.

271 Gingras, M.K., Bann, K.L., MacEachern, J.A., Waldron, J., Pemberton, S.G., 2007. A
272 Conceptual Framework for the Application of Trace Fossils. In: MacEachern, J.A.,
273 Bann, K.L., Gingras, M.K., Pemberton, S.G. (Eds.), *Applied Ichnology*. SEPM Society
274 for Sedimentary Geology 52, pp. 1–25.

275 Gingras, M.K., MacEachern, J.A., 2012. Tidal ichnology of shallow-water clastic settings. In:
276 Davis, Jr., Dalrymple, R.W. (Eds.), *Principles of Tidal Sedimentology*. Springer, pp. 57–
277 77.

278 Gingras, M.K., Zonneveld, J.-H., 2015. Tubular tidalites: A biogenic sedimentary structure
279 indicative of tidally influenced sedimentation. *Journal of Sedimentary Research* 85, 845–
280 854.

281 Gong, C., Wang, Y., Rebesco, M., Salon, S., Steel, R.J. 2018. How do turbidity flows interact
282 with contour currents in unidirectionally migrating deep-water channels? *Geology* 46,
283 551–554.

284 Gonthier, E., Faugères, J.-C., Stow, D.A.V., 1984. Contourite facies of the Faro Drift, Gulf of
285 Cadiz. In: Stow, D.A.V., Piper, D.J.W. (Eds.), *Fine Grained Sediments, Deepwater*
286 *Processes and Facies*. Geological Society, London, Special Publication 15, pp. 275–291.

287 Hubbard, S.M., MacEachern, J.A., Bann, K.L., 2012. Slopes. In: Knaust, D., Bromley, R. (Eds.),
288 *Trace fossils as indicators of sedimentary environments*. *Developments in*
289 *Sedimentology* 64, Elsevier, pp. 607–642.

290 Keighley, D.G., Pickerill, R.K., 1995. The ichnotaxa *Palaeophycus* and *Planolites*: historical
291 perspectives and recommendations. *Ichnos* 3, 301–309.

292 Knaust, D., 2017. *Atlas of trace fossils in well core. Appearance, Taxonomy and Interpretation*.
293 Springer, 209 pp.

294 Leonowicz, P., 2016. Tubular tempestites from Jurassic mudstones of southern Poland.
295 Geological Quarterly 60, 385–394.

296 Miguez-Salas, O., Rodríguez-Tovar, F.J., 2019. Stable deep-sea macrobenthic trace maker
297 associations in disturbed environments from the Eocene Lefkara Formation, Cyprus.
298 Geobios 52, 37–45.

299 Normandeau, A., Campbell, D.C., Cartigny, M.J.B., 2019. The influence of turbidity currents
300 and contour currents on the distribution of deep-water sediment waves offshore eastern
301 Canada. Sedimentology, doi: 10.1111/sed.12557

302 Osgood, R.G., 1970. Trace fossils of the Cincinnati area. Palaeontographica Americana 6, 193–
303 235.

304 Palamakumbura, R.N., Robertson, A.H.F., 2018. Pliocene–Pleistocene sedimentary–tectonic
305 development of the Mesaoria (Mesarya) Basin in an incipient, diachronous collisional
306 setting: facies evidence from the north of Cyprus. Geological Magazine 155, 997–1022.

307 Pemberton, S.G., Frey, R.W., 1982. Trace fossil nomenclature and the *Planolites-Palaeophycus*
308 dilemma. Journal of Paleontology 56, 843–881.

309 Pickering, K.T., Hiscott, R.N., 2016. Deep Marine Systems: Processes, Deposits, Environments,
310 tectonics and Sedimentation. American Geophysical Union and Wiley, 637 pp.

311 Rebesco, M., Hernández-Molina, F.J., Van Rooij, D., Wåhlin, A., 2014. Contourites and
312 associated sediments controlled by deep-water circulation processes: state of the art and
313 future considerations. Marine Geology 352, 111–154.

314 Rodríguez-Tovar, F.J., Uchman, A., 2004. Trace fossils after the K-T boundary event from the
315 Agost section, SE Spain. Geological Magazine 141, 429–440.

316 Rodríguez-Tovar, F.J., Hernández-Molina, F.J., 2018. Ichnological analysis of contourites: Past,
317 present and future. Earth-Science Reviews 182, 28–41.

318 Rodríguez-Tovar, F.J., Hernández-Molina, F.J., Hüneke, H., Llave, E., Stow, D., 2019a.
319 Contourite facies model: Improving contourite characterization based on the
320 ichnological analysis. Sedimentary Geology 384, 60–69.

321 Rodríguez-Tovar, F.J., Mayoral, E., Santos, A., Dorador, J., Wetzel, A., 2019b. Crowded tubular
322 tidalites in Miocene shelf sandstones of southern Iberia. Palaeogeography,
323 Palaeoclimatology, Palaeoecology 521, 1–9.

- 324 Sansom, P., 2018. Hybrid turbidite-contourite systems of the Tanzanian margin. *Petroleum*
325 *Geoscience*, doi:1100 <https://doi.org/10.1144/petgeo2018-044>
- 326 Shanmugam, G., 2002. Ten turbidite myths. *Earth-Science Reviews* 58, 311–341.
- 327 Stow, D.A.V., Shanmugam, G., 1980. Sequence of structures in fine-grained turbidites:
328 Comparison of recent deep-sea and ancient flysch sediments. *Sedimentary Geology* 25,
329 23–42.
- 330 Stow, D.A.V., Kahler, G., Reeder, M., 2002. Fossil contourites: Type example from an
331 Oligocene palaeoslope system, Cyprus. In: Stow, D.A.V., Pudsey, C.J., Howe, J.A.,
332 Faugères, J.-C., Viana, A.R. (Eds.), *Deep-Water Contourite Systems: Modern Drifts and*
333 *Ancient Series, Seismic and Sedimentary Characteristics*. Geological Society of London
334 *Memoir* 22, pp. 443–455.
- 335 Wanless, H.R., Tedesco, L.P., Tyrrell, K.M., 1988. Production of subtidal tubular and surficial
336 tempestites by Hurricane Kate, Caicos Platform, British West Indies. *Journal of*
337 *Sedimentary Petrology* 58, 739–750.
- 338 Wetzel, A., 2015. Burrows storing an otherwise lost sedimentary record. In: McIlroy, D. (Ed.),
339 *ICHNOLOGY: Papers from ICHNIA III*. Geological Association of Canada,
340 *Miscellaneous Publication* 9, pp. 211–224.
- 341 Wetzel, A., Carmona, N., Ponce, J.J., 2014. Tidal signature recorded in burrow fill.
342 *Sedimentology* 61, 1198–1240.
- 343 Wetzel, A., Werner, F., Stow, D.A.V., 2008. Bioturbation and biogenic sedimentary structures in
344 contourites. In: Rebesco, M., Camerlenghi, A. (Eds.), *Contourites. Developments in*
345 *Sedimentology* 60. pp. 183–202.

347 **Figure captions**

348

349 **Figure 1.** Location and geological map of the Petra Tou Romiou section (southern Cyprus)
350 (modified from Constantinou, 1995; Palamakumbura and Robertson, 2018).

351 **Figure 2.** General lithological column of the Petra Tou Romiou section with detailed of the
352 studied Chalk Unit showing regular alternation of calcilutites and calcarenite beds, including
353 outcrop photograph.

354 **Figure 3.** Detailed field photographs of the vertical calcilutite-calcarenite-calcilutite succession
355 showing different facies. These include whitish calcilutites (calu), well-developed calcarenite
356 beds (caln: continuous, caln-d; discontinuous), whitish calcarenites with faint wavy lamination
357 (calnwl), and whitish calcilutites. Note the horizontal lamination in the well-developed
358 calcarenite bed shown in panel D.

359 **Figure 4.** Trace fossils observed in calcilutite intervals below a well-developed, continuous
360 calcarenite bed (black arrow). These include a light-colored trace fossil assemblage with
361 calcilutite infill similar to the host sediment (light green arrows; *Ch*: *Chondrites*, *Pl*: *Planolites*,
362 *Th*: *Thalasinoides*, and *Zo*: *Zoophycos*) and a trace fossil assemblage consisting of calcarenite
363 infill similar to the calcarenite beds (yellow arrows; *Pl*: *Planolites*).

364

365 **Figure 5.** Field photographs of differentiated cases (i to iii) showing varying relationships
366 between conspicuous calcarenite filled traces and overlying sharp based calcarenites. Case i (**A**,
367 **B**): Conspicuous calcarenite filled trace fossils (blue arrows) in contact with (**B**) or at a short
368 distance from (**A**) a well-developed, continuous calcarenite bed (black arrow; caln). Case ii (**C**,
369 **D**, **E**) Conspicuous calcarenite filled trace fossils (blue arrows) at a short distance from a
370 discontinuous calcarenite horizon (**C**, **D**, caln-d) or pressure dissolution seam (**E**, red arrow;
371 pds). Note calcilutite infilled trace fossils (yellow arrows) in D. Case iii (**F**): Conspicuous
372 calcarenite filled trace fossils (blue arrows) bioturbating the calcilutite interval (calu) lacking
373 evidence of a calcarenite bed/horizon or a pressure dissolution seam.

374

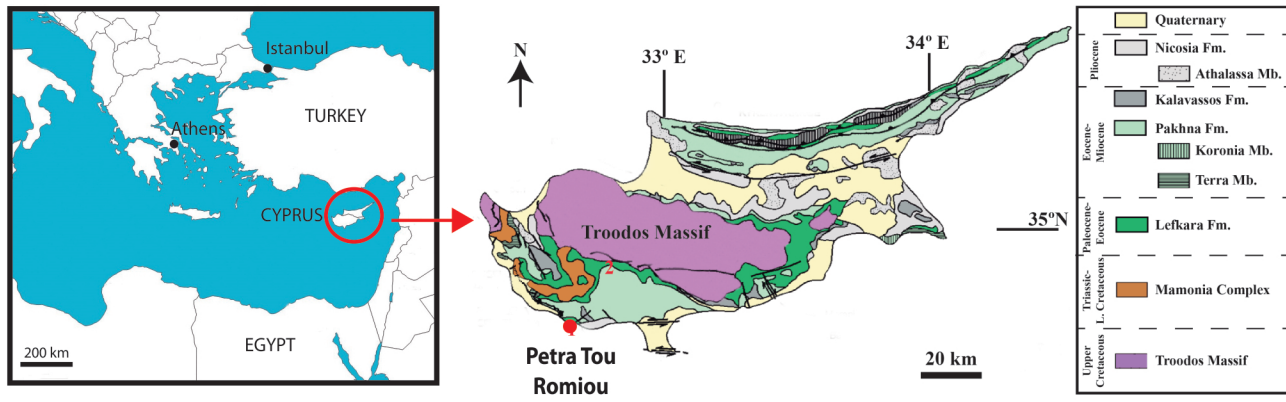
375 **Figure 6.** Sketch summarizing tubular turbidites models (bypass vs erosion). Above: *Tubular*
376 *turbidites* – bypass model (Hubbard et al., 2012): A) Firm ground *Thalassinoides* previous to
377 turbiditic event in fine-grained pelagic sediment, B) Passive infilling of *Thalassinoides* by
378 coarser-grained sediment during turbiditic event, C) Tubular turbidites (*Thalassinoides*) after
379 bypass of turbiditic event, D) Deposition of fine-grained pelagic sediment. Below: *Tubular*
380 *turbidites* – erosion model: A) Fine-grained pelagic sediment, B) Coarse-grained turbiditic event,
381 C) Bioturbation of active infilling *Planolites* in softground coarse-grained turbiditic sediment, D)
382 *Tubular turbidites* (*Planolites*) after erosion of coarse-grained turbiditic sediment and deposition
383 of fine-grained pelagic sediment.

384 **Figure 7.** Sketch summarizing different cases of turbiditic and bottom-current interactions (cases
385 i to iii), according to the magnitude of post-depositional erosion of turbiditic calcarenite material
386 by bottom-current activity. Note the variable relationship between pelagic calcilutites, well-
387 developed calcarenite beds, and whitish calcarenites with faint wavy lamination, and the
388 relationship with conspicuous traces with calcarenite infill. Note: Fig. 3 caption describes facies
389 types.

390

391

Figure 1



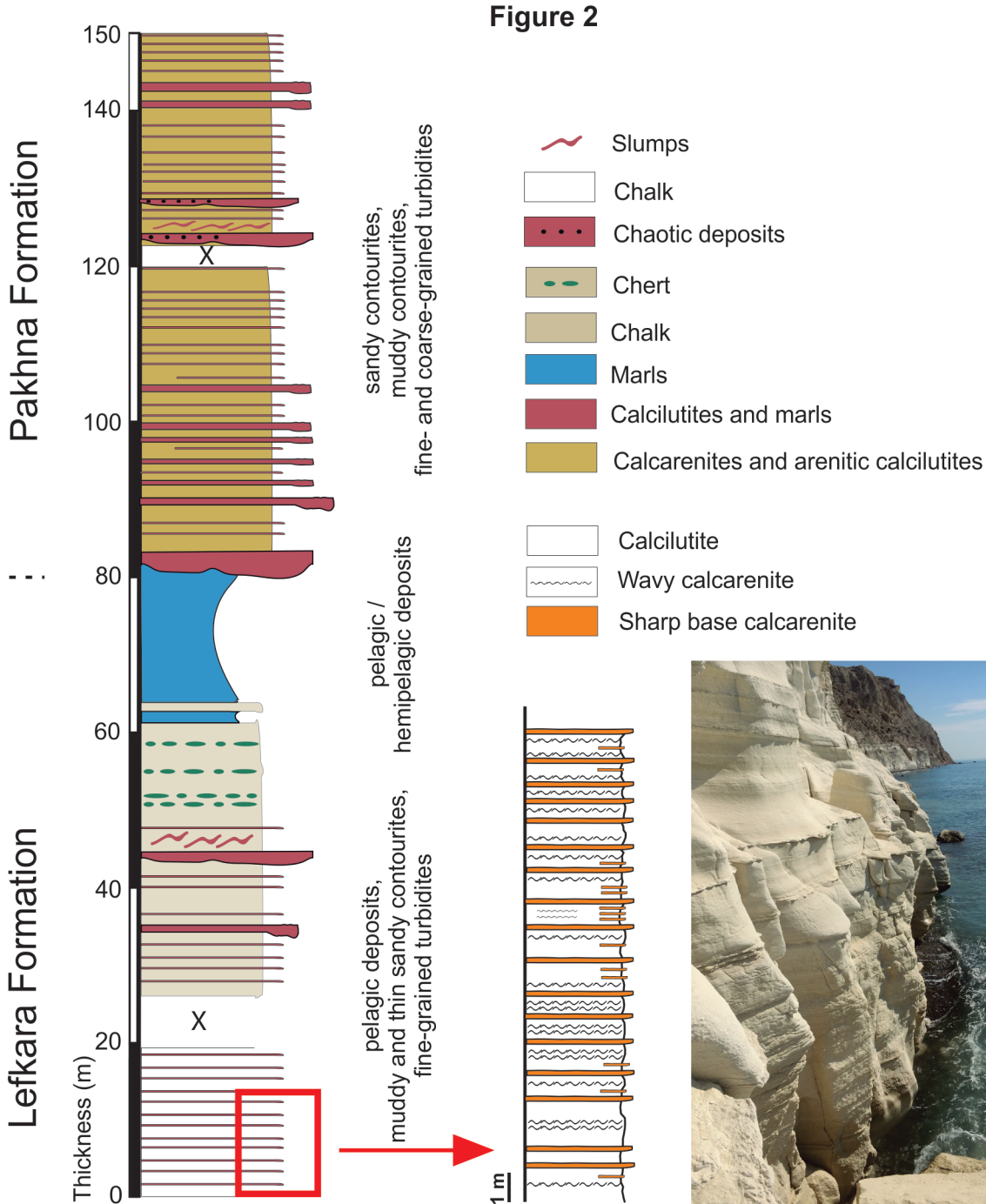


Figure 3

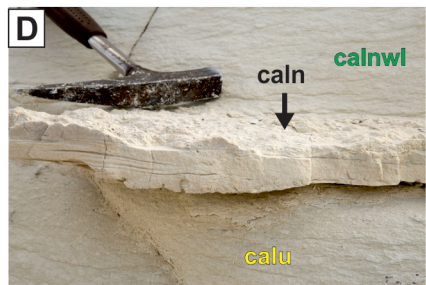
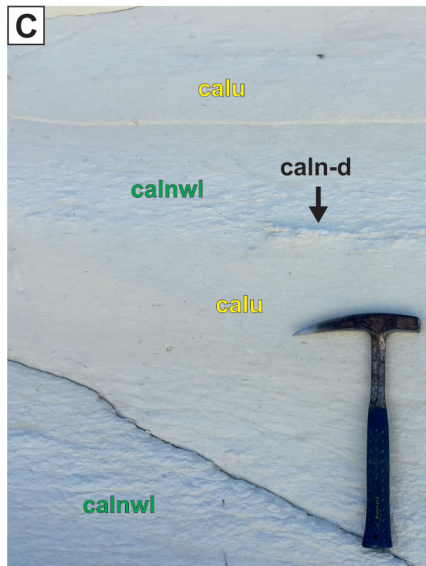
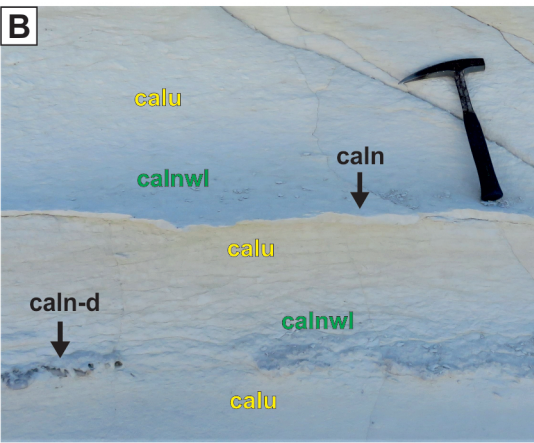
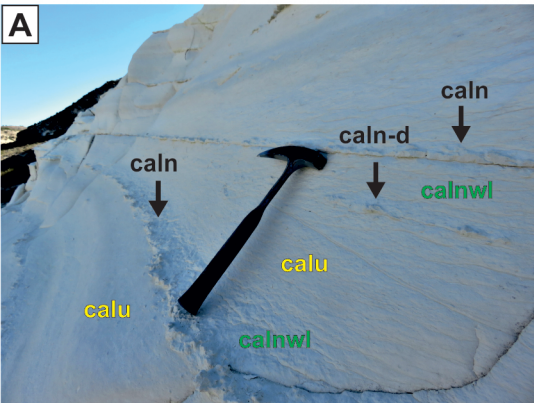


Figure 4

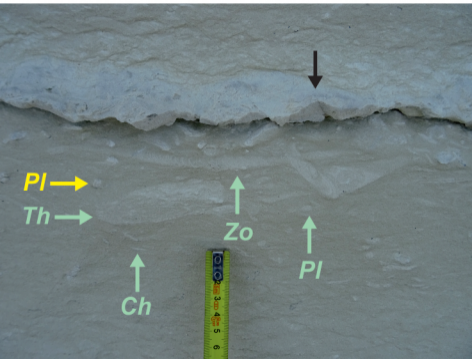


Figure 5

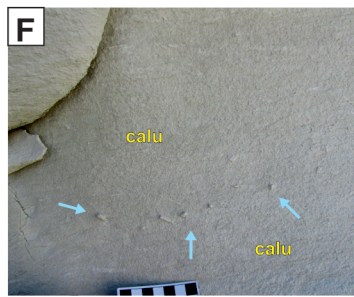
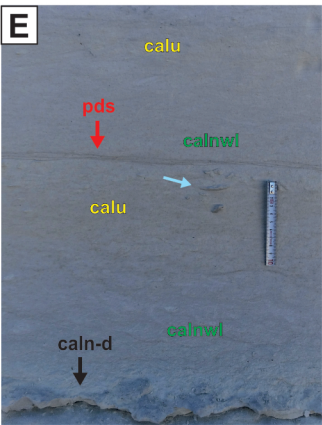
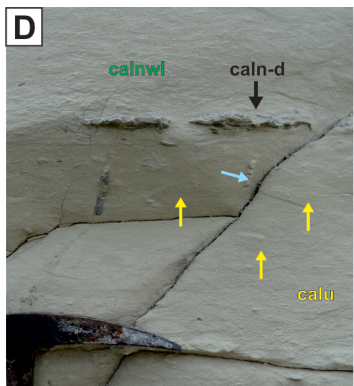
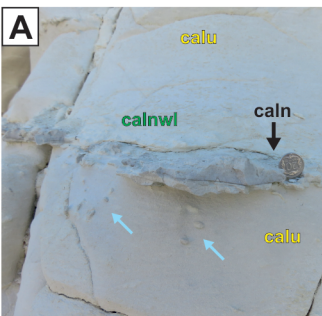
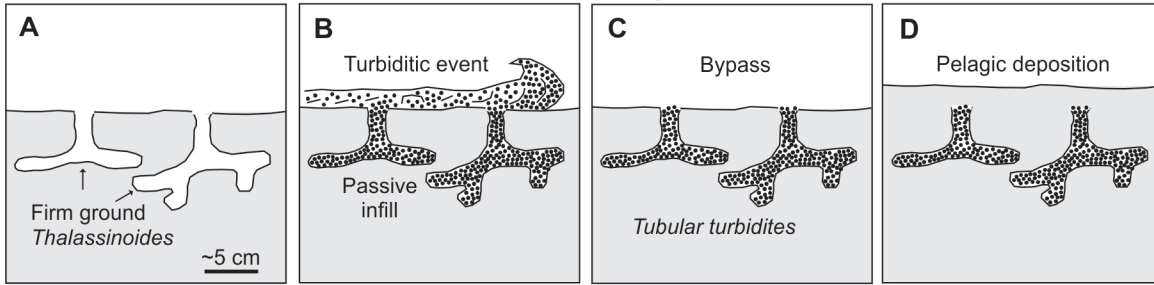


Figure 6

Tubular turbidites - bypass model



Tubular turbidites - erosion model

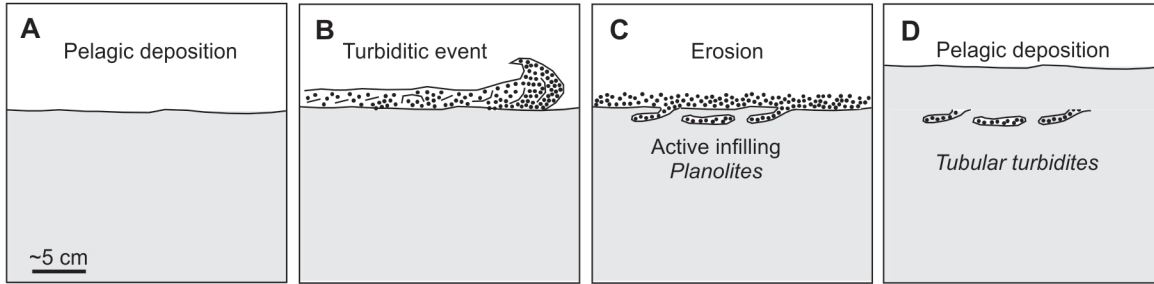
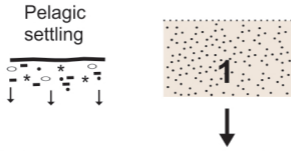


Figure 7

1- Pelagic deposition of lower calcilutitic interval



2- Turbidite deposition & bioturbation of calcarenite bed

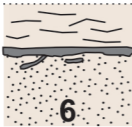


Bottom current



3- Absence/scarce pelagic sedimentation: increase firmness

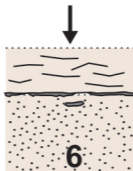
6- Contourrite deposition of calcarenites with wavy lamination



7- Pelagic deposition of upper calcilutitic interval



4- Minor erosion: thin calcarenite horizon and infilled traces



5- Major erosion: tubular turbidites

